PARTICLE MOTIONS IN UNDERWATER SOUND FIELDS

Jens M Hovem Norwegian University of Science and Technology
Department of Electronics and Telecommunications/ Acoustics
Trondheim, Norway, hovem@iet.ntnu.no

1 BACKGROUND AND MOTIVATION

There are increasing concerns about the impact of anthropogenic acoustic noise in the oceans since such noise may have a significant impact on aquatic life and ecosystem[1,2,3]. This particular work is motivated by the impact acoustic noise may have on commercial fishing. It is well known that fishing vessels self-noise may have affect catches and that some vessels are known to be more successful than other vessels.

The frequency and levels of acoustic noise that may result in a change of behaviour and possible escape reactions depends on the species. Figure 1 shows auditory and startle threshold for Atlantic cod[4]. The frequency range of maximum sensitivity for this specie is in the frequency range of 30 Hz to 300 Hz and the level difference between hearing the noise and startling response is more than 80 dB. Figure 1 also shows measured high-resolution frequency spectrum of a large Norwegian trawler[5] having spectrum peaks at the low frequency range of maximum hearing sensitivity of cod.

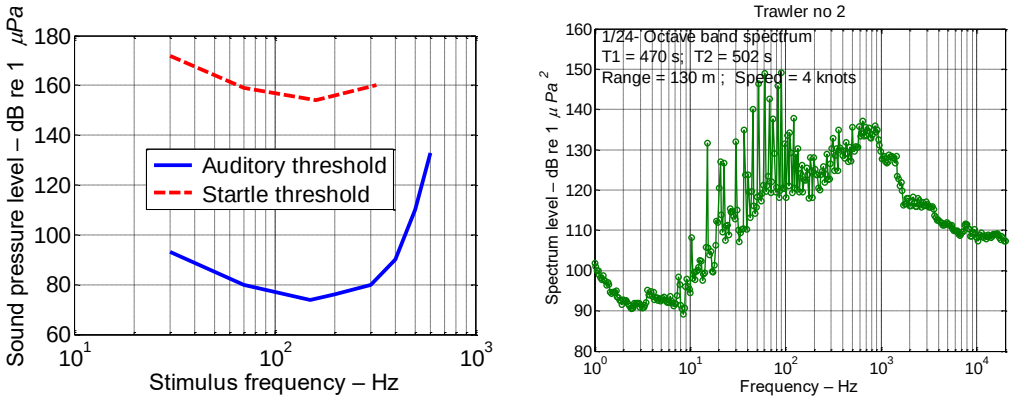

Figure 1 (Left) Hearing thresholds for Atlantic cod Sound pressure level
(Right) measured noise spectrum of a trawler as function of frequency with referece to a distanc of one meter

Figure 1 represents the conventional view; the thresholds are specified in terms of sound pressure. However, marine biologist have found that many aquatic animals sense sound using particle motions, some in addition to sound pressure. Therefore, particle motions of sound field needs to be included when addressing the effects of sound on fishes. Traditionally, measurements and modelling of ocean acoustic wave fields have only been concerned with sound pressure and not on particle motion, which is vector quantity and more difficult to measure and model [6]. The purpose of this paper is to present a modelling technique for particle movements of underwater sound fields.

2 MODELLING PARTICLE MOTIONS USING RAY THEORY

The method for modelling particle movements of acoustic fields is based on decomposition of a wave field into a sum of eigenrays or multipath contributions, each being plane waves having the property that the particle velocity is the sound pressure divided by the specific acoustic impedance. Knowing also the directions of each eigenray, the horizontal and vertical components are determined. The core of this model is an efficient algorithm for finding eigenrays in scenarios with arbitrary sound speed profile and range dependent bathometry.

2.1 Theoretical Background

The solution of the acoustic wave equation for a waveguide can be expressed by the equation[7,8]

$$\Psi(r,z,\omega) = \frac{1}{4\pi}\int_0^\infty S(\omega)\Phi\left(k,z,\omega\right)H_0^{(1)}(kr)kdk. \qquad (1)$$

Ψ(r, z, ω) is the acoustic field as function of positon *r* and *z* and ω is (angular) frequency. The integration is over the horizontal wave number *k* and the integrand is given by the source function *S*(ω) and the Hankel function $H_0^{(1}$(*kr*). The environmental function, Φ(*k, z,* ω), is the solution of the depth separated wave equation containing the effects of sound speed profile and reflections and interactions with the sea surface and the bottom. A fundamental condition for this solution is that the environment is constant in range, i.e. the water depth, the bottom and the sound speed are range independent.

Equation (1) gives the field as integral of plane waves the integral to be over all values of the wavenumber *k*. Since *k*=(ω/*c*) cos α, the integral includes all initial angels α, also the imaginary angles occurring when *k* > ω/*c*). At long ranges the Hankel functions can be approximated to

$$H_0^{(2)}\left(kr\right) \approx \sqrt{\frac{2}{\pi kr}}\exp\left(-ikr + i\frac{\pi}{4}\right), \qquad (2)$$

which is a plane wave propagating in the positive *r* direction.

There are several ways of evaluating equation (1) in, but this paper considers only:

1. Evaluation by numerical integration, which leads to the wave number integration technique
2. Expansion using the method of stationary phase, which leads to the ray-tracing approach.

The wave number integration technique is direct numerical evaluation of the integrand by discretization and summing. Examples of using the approach will be treated later in this paper.

Another approach, which is the focus of this paper, is using ray theory and decomposition of the wave field into a sum of eigenrays or multipath contributions; each being plane waves having the property that the particle velocity is the sound pressure divided by the specific acoustic impedance.

2.2 Plane Ray model

The propagation model PlaneRay, Hovem[8,9] is a ray theory model that can deal with range dependent bathymetry and the bottom can be layered, for instance with a sedimentary sediment layer over solid rock. The unique feature of PlaneRay is an efficient algorithm for finding eigenrays connecting a source with a receiver at arbitrary positions. The program first computes the trajectories of a large number of rays with the starting angles at the source covering the total water volume in range and depth of interest to the analysis. The locations and striking angles of all surface and bottom reflections are noted and geometrical transmission loss are computed.

All this is information is stored in the computer memory in tables of ray history. Then the eigenrays to a particular point in space are found by look-up, sorting and interpolation in the stored ray history.

Figure 2 shows examples for an undulating up-sloping bottom having for two sound speed profile for typical northern waters. The figure shows ray trajectories from a source at 5 m depth with initial angles spanning the angular range from -60º to +60º.

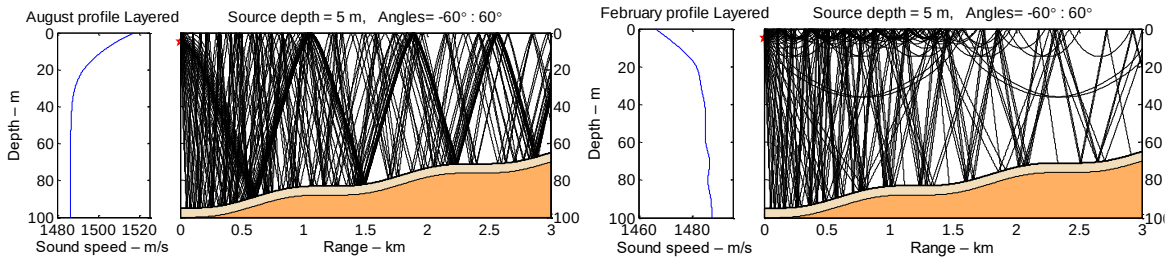

Figure 2 Sound speed profile and ray traces for summer (August) winter (February) conditions.

2.3 Bottom and surface reflectivity

The reflection coefficient of the sea surface is set to -1, but surface roughness caused by ocean waves is included using the incoherent reflection loss of the Rayleigh formulation as function of rms. roughness, frequency and incident angle. Incoherent reflection loss of a rough bottom is treated in the same way.

At low frequencies, relevant for low frequency applications of this study, the geoacoustic properties of the seafloor is very important. Figure 3 shows an example of the bottom reflection loss, in dB, as function of grazing angle and frequency. The bottom has a fluid sediment layer with thickness *d* over an elastic halfspace. The sound speed and density of the sediment layer is 1700 m/s and is 1500 kg/m^3, respectively. The elastic half-space is a hard bedrock with compressional speed of 3000 m/s and shear speed 500 m/s and with density of 2000 kg/m^3. All wave attenuations are set to 0.5 dB per wavelength. The vertical axis is the product of layer thickness and the frequency, $X = d \cdot f$. At the lowest frequency- thickness values, the bottom behaves as a solid, since the sediment layer appears to be very thin. At higher frequencies, the sediment layer appears to be thick and the bottom reflectivity is primarily determined by the properties of the sediment layer. The effect of this is that the critical angle charges from about 60° at low frequency to about 28° at higher frequency.

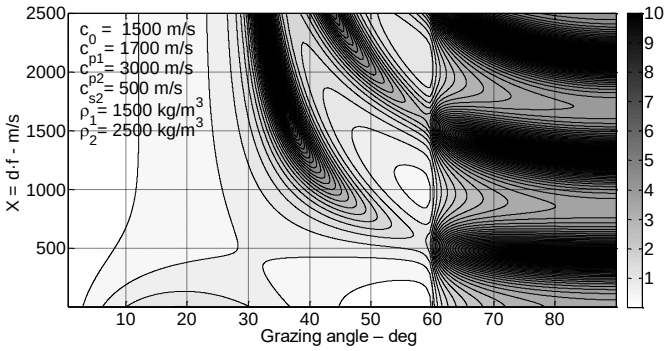

Figure 3 Bottom reflection loss in dB as function of grazing angle and the product of frequency and layer thickness.

2.4 Modelling particle velocity

The complete history of the initial raytracing is stored in a file, called *HIST*, such that the sound pressure can be expressed symbolically as

$$p(r,z,\omega) = \sum_{n=1}^{N} HIST\left(r,z,\omega\right) \tag{3}$$

The horizontal and vertical components of the particle velocities are obtained taking into account the angels of the eigenrays at the receiver, the angles β_n

$$\begin{aligned} u_{hor}(r,z,\omega) &= \frac{1}{\rho c}\cdot\sum_{n=|}^{N} HIST_n\left(r,z,\omega\right)\cos\left(\beta_n\right) \\ u_{ver}(r,z,\omega) &= \frac{1}{\rho c}\cdot\sum_{n=|}^{N} HIST_n\left(r,z,\omega\right)\sin\left(\beta_n\right) \end{aligned} \tag{4}$$

In addition, it is useful to introduce a nominal particle velocity as

$$u_{nom}(r,z,\omega) = \frac{1}{\rho c}\cdot\sum_{n=|}^{N} HIST_n\left(r,z,\omega\right) \tag{5}$$

This velocity is useful as a reference and is obtained by taking a measured or modelled sound pressure and divide with the acoustic impedance. Equations (4) and (5) imply that both the amplitudes of the vertical and the horizontal particle velocities are weaker than the nominal particle velocity.

Figure 4 displays parts of the ray history as function of initial angle at the source. The two plots show ranges and travel times to locations where the rays cross the receiver depth-line, which in this case is at a depth of 50 m. The initial angles at a particular define the eigenrays. The trajectories of some of the eigenrays are shown in Figure 5 for a position of 2 km from the source.

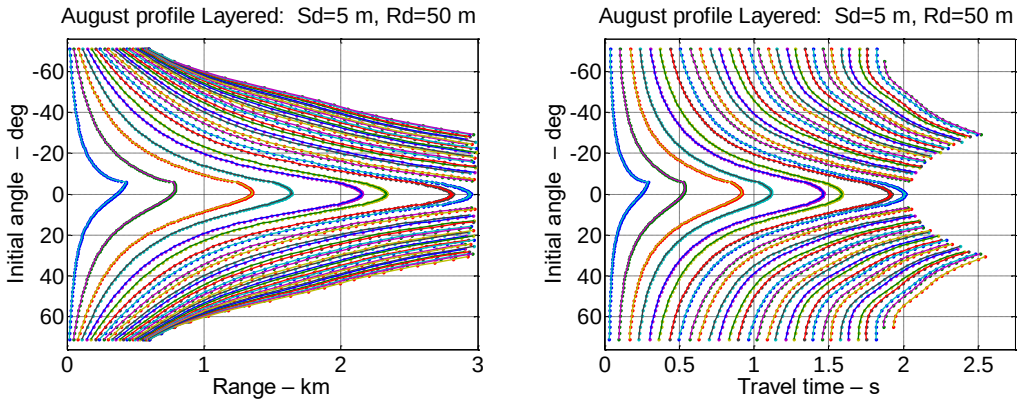

Figure 4 Ray history of rays in Figure 1 showing range (left) and travel time (right) as function of initial angles at the source.

The acoustic intensity $I(r)$ as function of horizontal range is, according to this principle, given by

$$I(r) = I_0 \frac{r_0^2}{r} \frac{\cos\alpha_0}{\sin\beta} \left| \frac{d\alpha_0}{dr} \right| \quad . \tag{6}$$

Here α_0 is the initial launch angle at the source and β is the ray angle at the receiver point.

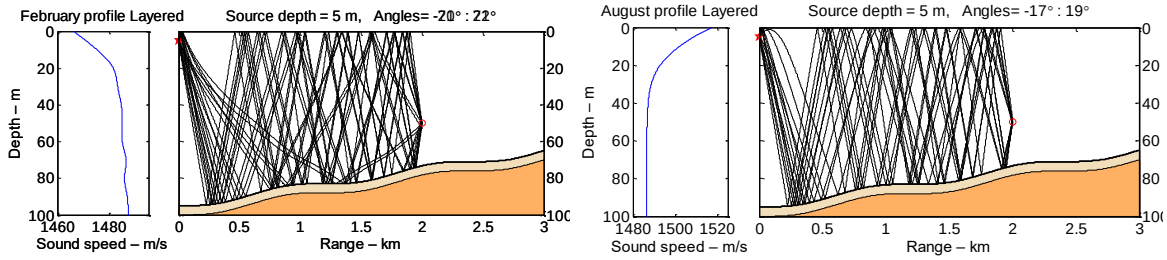

Figure 5 Eigenrays to a receiver position at depth 50 m and range of 2km

Figure 6 exhibits the impulse responses of the eigenrays as function target angle and travel time for a frequency of 100 Hz. Positive angles signifies rays coming from above and negative angles are rays going upwards. The calculation is for a layer thickness of 5 m and the frequency of 100 Hz. With these values, the critical angle is about 60° according to Figure 3 and the amplitudes of eigenrays with angle steeper angles are very weak. The plot of arrival times shows that the received signal are a series of pulses over a duration of time of ca 200 ms in this example.

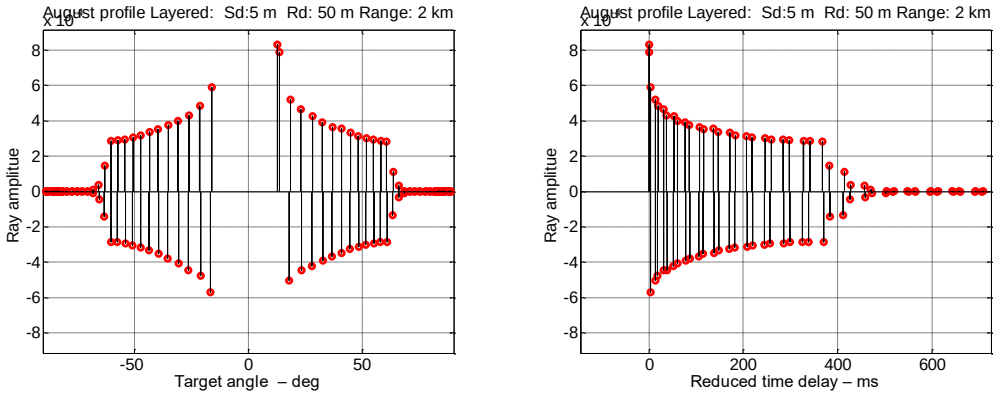

Figure 6 Impulse responses as function of target angle and travel times at 100 Hz. August sound speed profile, layered bottom and frequency 100 Hz

Time responses of the received signals are obtained by convolving the impulse response with a source function. To illustrate the structure of the time signal a short impulsive source is used in the following examples. The source signal is a Ricker pulse with peak frequency of 100 Hz and time duration of about 2 ms.

Figure 7 shows the received time responses with amplitudes, (in *μm/s)*, at ranges of 500 m and 1000 for the nominal and vertical and horizontal particle velocities calculated for a source pulse with peak pressure of 200 dB re 1 *μPa.* The received signals are a sequence of short pulses separated over time interval increasing with range. Figure 8 shows how the same received signals evolve with range.

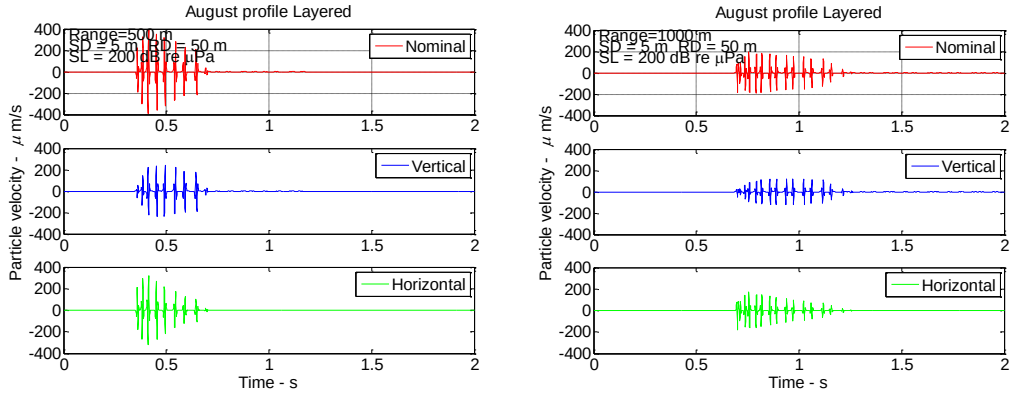

Figure 7 Time functions of particle velocities at distances of 500 m and 1000 m

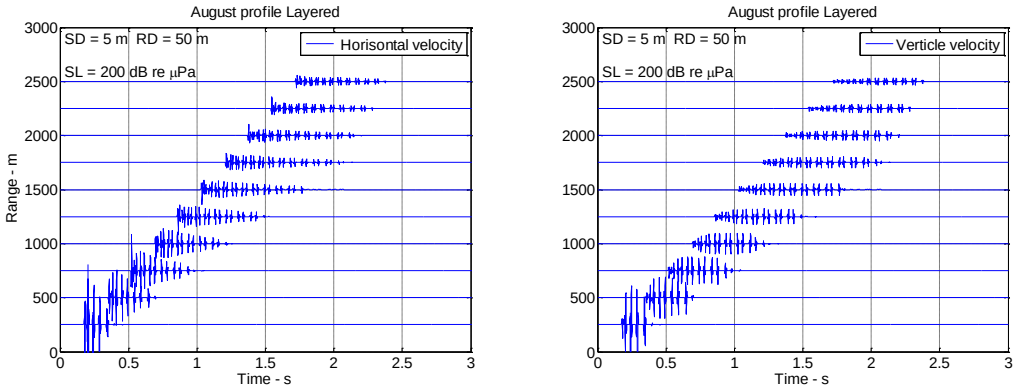

Figure 8 Time functions of particle velocities as function of distance

3 ENVIRONMENTAL EFFECTS

Models are useful for obtaining knowledge on how different environmental conditions may affects an acoustic field. This illustrated by an example using a winter (February) sound speed profile and a soft bottom with sound speed of 1700 m/s. The significant eigenrays contributions are limited to rays striking with angles less than the bottom critical angle- In the case of a soft bottom the with sound speed of 1700 m/s the critical angle about 28°. Figure 9 shows the channel impulse response for this case and, and figure 10, and 11 show the time response to a Ricker source pulse.

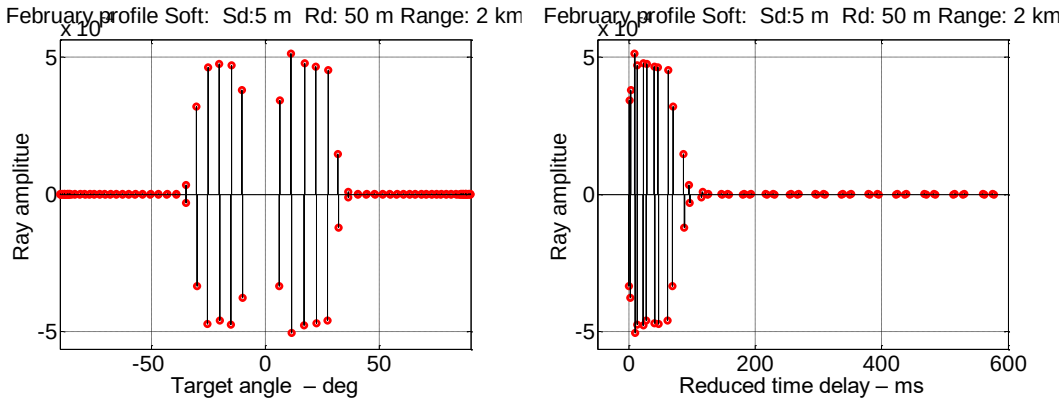

Figure 9 Impulse response as function of target angle for and travel times. February sound speed profile, soft bottom and frequency 100 Hz

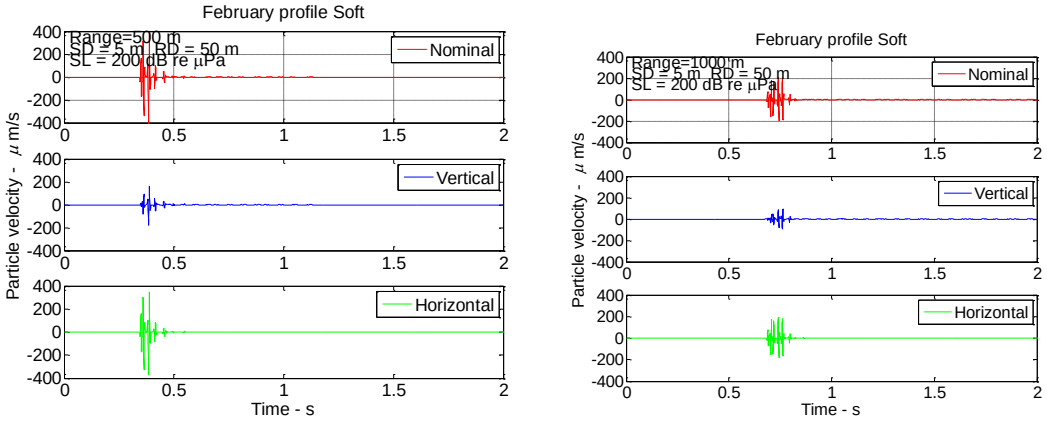

Figure 10 Time functions of particle velocities at distances of 500 m and 1000 m

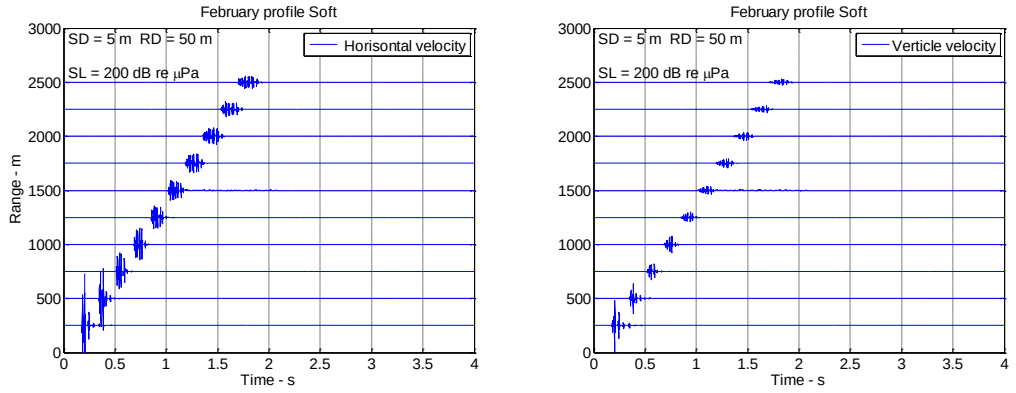

Figure 11 Time functions of particle velocities as function of distance

4 VALIDITY AND LIMITATIONS OF RAY MODELLING

Ray theory is often believed to be valid only for high frequency application, but this is too simplistic view as can be demonstrated by comparison with the wave number integration model OASES[10]. In Figure 12, the transmission loss of PlaneRay is compared with OASES for a Pekeris waveguide with constant water depth of 100 m and sound speed of 1500 m/s. The source is at 5 m and the receiver at 96 m depth. The bottom is a layered with a 5 m thick sediment layer over a solid halfspace with reflection loss as in Figure 3. Figure 12 shows that the transmission loss calculated by the two codes are very close with only minor deviations at the frequency of 25 Hz.

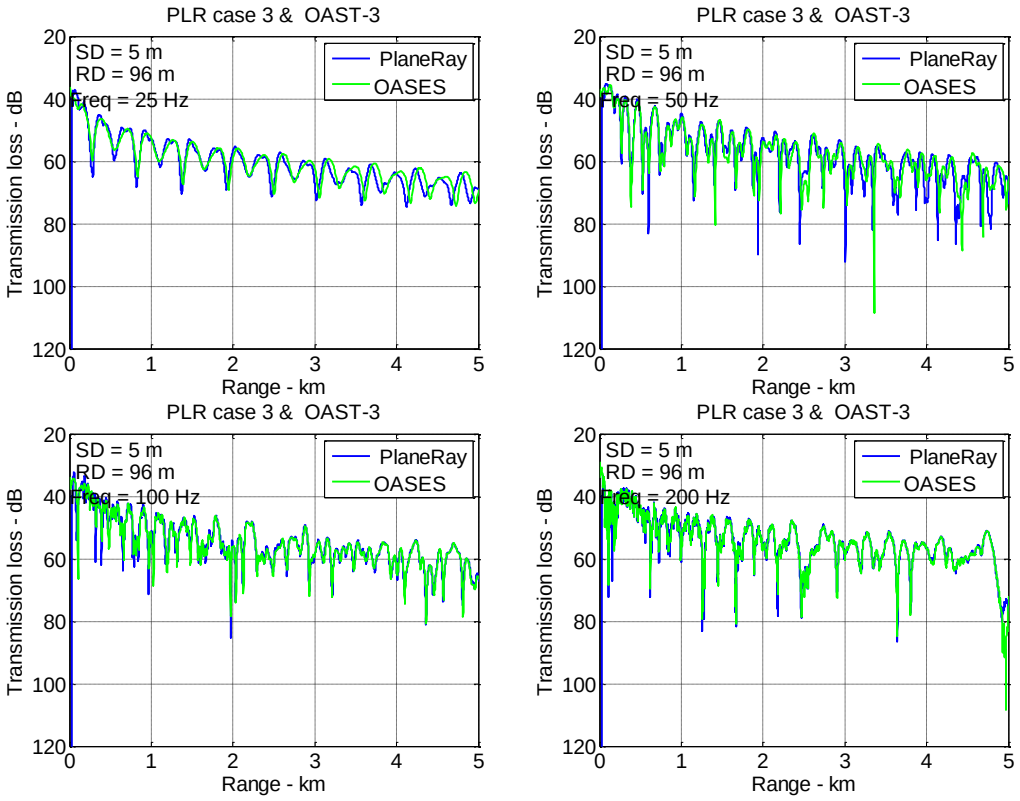

Figure 12 Comparison of the transmission loss as function of range and frequency by PlaneRay and OASES for a Pekeris' waveguide with a sedimentary layer over a solid half space

4.1 Source and receivers close to the bottom at low frequencies

The ray model appears to produce accurate for the cases considered so far. However, limitations exists, in particular for very low frequencies and with both source and receiver are close to a solid elastic bottom. As indicated in the discussion of equation (1), the complete solution requires integration over all wave numbers, also the wave number corresponding to imaginary angles. These contributions are not included by ray theory and therefore ray models miss refracted waves and interface waves, also called Scholte waves. These waves propagate along the interface with a speed of nearly the speed of the shear speed and decaying exponentially with the distance from the interface. These components may be important for studies of very low sound, for instance studies of impact noise of piling work and its impact on the aquatic life on the bottom. This problem has been are treated by Hovem[11], and in more details, by Hazelwood and Macey[12].

Figure 13 shows the integrand of equation(1) for a case with a source is five m and a receiver is one meter above an elastic bottom. The bottom compressional wave speed is 2000 m/s, shear speed 400 m/s and density of 2000 kg/m. For any frequency, the integrand yields two main of contributions. The first represents the reflected wave travelling with the sound speed of the water (There may also be a small contribution of refracted waves, but too small to be seen.) The second main contribution is the Scholte interface wave travelling with a speed slightly below the shear speed of the bottom.

Figure 14 shows the time responses obtain by OASES for a 5 Hz Ricker source pulse. The slow interface wave are present in all components These responses are for the low source frequency 5Hz, for higher frequencies as used in the previous other examples, the slow interface components of would be significantly reduced. Figure 15 shows the time responses calculated for the case that the bottom shear speed is set to zero. This is the same result as obtained with the ray model. The vertical component of the particle velocity is very weak.

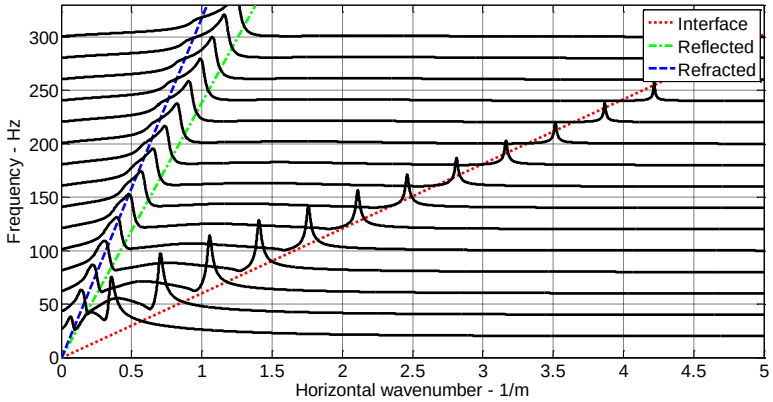

Figure 13 The integrand as function of horizontal wave number

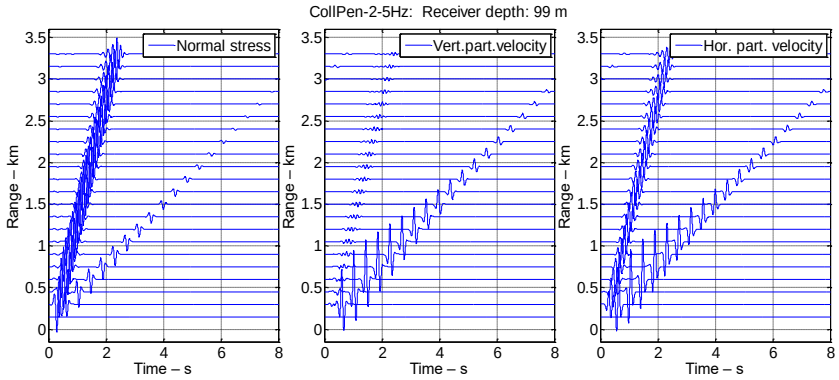

Figure 14 Time responses of normal stress, vertical and horizontal particle velocities when shear conversion is included

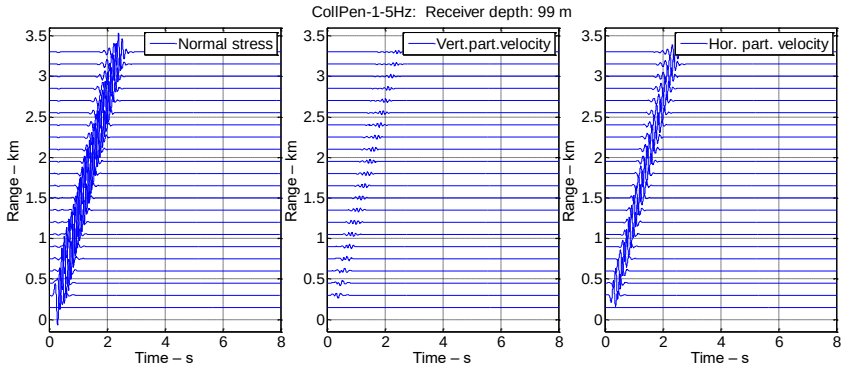

Figure 15 Time responses of normal stress, vertical and horizontal particle velocities when shear wave conversion is neglected

5 SUMMARY AND CONCLUSIONS

The model for calculating horizontal and vertical particle velocities of acoustic fields is based on ray theory and decomposition of the field into a sum of eigenray contributions, each being plane waves. The model uses an effective algorithm for finding eigenrays and eigenangles at any receiver positions

The horizontal and vertical particle motions are dependent on the angles of the eigenrays and for transmission over distances longer that the water depth the angles are limited by the critical angle of the seabed. Only rays striking the bottom with angles lower than the bottom critical angles give significant contribution to the acoustic fields at long ranges.

In any case, the amplitudes of the vertical and the horizontal particle velocities are weaker than the nominal particle velocity found by taking the total sound pressure and dividing with the acoustic impedance. Furthermore, most seabed have critical angles lower than 20° for a sediment bottom and 60° for hard bottom. This means the amplitudes of the vertical particle velocity is, at most, about 50% of the nominal particle velocity.

The validity and limitations of the model are evaluated by comparing with the wavenumber integration code OASES for range independent cases showing that the ray model is valid for most case relevant to fishing. The exception are for very low frequencies and bottom of solid rocks that can support shear wave propagation. With source and receiver close to the bottom, the ray mode fails because interface waves are not include. These components may be important for studies of very low frequency sound, for instance studies of noise of piling work and its impact on aquatic life on the bottom.

6 REFERENCES

1. Popper, A.N and Hastings, M. C. The effects of anthropogenic sources of sound on fishes. Journal of Fish Biology vol. 75, 455-489, (2009)
2. Popper, A. N. and Fay R.R. Rethinking sound detection by fishes. Hearing Research 273 (2011) 25-36.
3. Chapman, C. J. and A. D. Hawkins, (1973) A field study of hearing in the cod, Gadus morhua. L. J. Comp. Physiol., vol. 85: p. 147-167.
4. Karlsen, H. E., W. Piddington, P. S. Enger, and O. Sand, Infrasound initiates directional fast-start escape responses in juvenile roach Rutilus rutilus. J. Exp. Biol., 2004. 2007(4185-4193).
5. Private communication, Ecoxy AS.
6. Nedelec, S.L., Campbell, J., Radford, A. N., Simpson, S. D., and Merchant, N.D. Particle Motion: the missing link in underwater acoustic ecology. In Methods in Ecology and Evaluation 2016. https://www.researchgate.net/publication/292677434
7. Jensen F. B., W. A. Kuperman, M. B. Porter, and H. Schmidt, Computational Acoustics, AIP Press, New York Jersey, (1993).
8. Hovem, Jens M., Marine Acoustics –The Physics of Sound in Underwater Environments, Peninsula Publishing, Los Altos CA, USA 2012.
9. Hovem, Jens M. "Ray Trace Modeling of Underwater Sound Propagation," in Modeling and Measurement Methods for Acoustic Waves and for Acoustic Microdevices, InTech, Rijeka, Croatia, [2013]. ISBN 978-953-51-1189-4.
10. Schmidt H., SAFARI. Seismo-acoustic fast field algorithm for range independent environments. User's guide, SR-113, SACLANT Undersea Research Centre, La Spezia, Italy (1987).
11. Hovem, Jens M, Sound propagation over an elastic bottom – Particle motions caused by seismic interface waves, 2st Underwater Acoustics Conference and Exhibition, 22nd to 27th June 2014, Rhodes, Greece, [2014].
12. Hazelwood, R., A. and P.C. Macey, Modeling water motion near seismic waves propagating across a graded seabed as generated by man-made impacts. J. Mar Sci. Eng. 2016,4.